Published in final edited form as:
Invest Ophthalmol Vis Sci. 2007 May ; 48(5): 2050–2061. doi:10.1167/iovs.06-0998.

Comparative Analysis of Human Conjunctival and Corneal Epithelial Gene Expression with Oligonucleotide Microarrays

Helen C. Turner[1], **Murat T. Budak**[2], **M. A. Murat Akinci**[1], and **J. Mario Wolosin**[1,3]

[1] Department of Ophthalmology, Mount Sinai School of Medicine, New York, New York

[3] Black Family Stem Cell Institute, Mount Sinai School of Medicine, New York, New York

[2] Pennsylvania Muscle Institute, University of Pennsylvania, Philadelphia, Pennsylvania

Abstract

Purpose—To determine global mRNA expression levels in corneal and conjunctival epithelia and identify transcripts that exhibit preferential tissue expression.

Methods—cDNA samples derived from human conjunctival and corneal epithelia were hybridized in three independent experiments to a commercial oligonucleotide array representing more than 22,000 transcripts. The resultant signal intensities and microarray software transcript present/absent calls were used in conjunction with the local pooled error (LPE) statistical method to identify transcripts that are preferentially or exclusively expressed in one of the two tissues at significant levels (expression >1% of the β-actin level). EASE (Expression Analysis Systematic Explorer software) was used to identify biological systems comparatively overrepresented in either epithelium. Immuno-, and cytohistochemistry was performed to validate or expand on selected results of interest.

Results—The analysis identified 332 preferential and 93 exclusive significant corneal epithelial transcripts. The corresponding numbers of conjunctival epithelium transcripts were 592 and 211, respectively. The overrepresented biological processes in the cornea were related to cell adhesion and oxiredox equilibria and cytoprotection activities. In the conjunctiva, the biological processes that were most prominent were related to innate immunity and melanogenesis. Immunohistochemistry for antigen-presenting cells and melanocytes was consistent with these gene signatures. The transcript comparison identified a substantial number of genes that have either not been identified previously or are not known to be highly expressed in these two epithelia, including testican-1, ECM1, formin, CRTAC1, and NQO1 in the cornea and, in the conjunctiva, $sPLA_2$-IIA, lipocalin 2, IGFBP3, multiple MCH class II proteins, and the Na-Pi cotransporter type IIb.

Conclusions—Comparative gene expression profiling leads to the identification of many biological processes and previously unknown genes that are potentially active in the function of corneal and conjunctival epithelia.

During the past decade, high throughput, high-density DNA microarrays have emerged as an efficient, powerful tool for providing useful information in the analysis of the global gene expression patterns in various tissues or biological systems.[1–3] At the ocular surface, such studies have been performed in the corneal epithelium in the context of disease (e.g.,

Corresponding author: J. Mario Wolosin, Department of Ophthalmology, Mount Sinai School of Medicine, 100th Street and 5th Avenue, New York, NY 10029-6574; jmario.wolosin@mssm.edu.

Disclosure: **H.C. Turner**, None; **M.T. Budak**, None; **M.A. Murat Akinci**, None; **J.M. Wolosin**, None

diabetes) or growth conditions.[4,5] The corneal (Co) and conjunctival (Cnj) epithelia are the main cellular components of the ocular surface.

These two distinct lineages derive from a small cohort of head ectodermal cells that become PAX6 positive at a relatively early developmental stage, before optical vesicle formation and organogenesis.[6–8] Both ocular surface epithelia are stratified and nonkeratinizing and display a wet phenotype that comprises multiple secretory and absorptive features related to the phenotypes of simple epithelia. They functionally combine to establish the protective and light refractory properties of the ocular surface. Unlike the keratinizing epidermis, these epithelia constitutively express PAX-6 throughout life. Given the common developmental origin and a degree of structural similarity between corneal and conjunctival epithelia, it appears logical that identification of genes that are uniquely or preferentially expressed in either of these two lineages will provide clues to the mechanisms that specifically underlie each phenotype and distinguish one from the other.

Accordingly, in this study, we used a large oligonucleotide array system, representing more than half of the known human genes, to compare the molecular signatures of these two tissues. Approximately one half of the genes represented in the array are expressed in either the corneal or conjunctival systems. Ninety percent of the transcripts present in one of the systems are also present in the other at a comparable level of expression. The remaining 10% represent genes that are present in only one of the tissues or are expressed at substantially higher levels in one epithelium over the other.

Materials and Methods

Tissue Procurement and Processing

Whole human conjunctivae and human corneas were obtained from the National Disease Research Interchange (NDRI, Philadelphia, PA) and processed between 48 and 72 hours of death. No donor details apart from age, sex, and cause of death were released. The criteria for tissue acceptance and inclusion were donor ages between 25 and 65 years (irrespective of sex) and overt physical integrity of the epithelium over the central cornea, as revealed by trypan blue stain. Conjunctivae and whole corneas that excluded an outer strip of limbus (to ensure that the sample contains no cells derived from the adjacent conjunctiva) were quartered and incubated overnight at 4°C in conical tubes containing 5 mL of 0.5% Dispase dissolved in 1:1 Dulbecco's modified minimal essential medium-Ham F-12 mix with slow (~20 cycles/min) end-to-end rocking. This treatment results in the spontaneous separation of intact epithelial sheets from the underlying stroma. The use of human tissue in the study was in accordance with the provisions of the Declaration of Helsinki and was sanctioned by the local Institutional Review Board.

RNA Preparation and Analysis

Epithelial sheets were manually transferred from the Dispase solution directly into lysis buffer, and total RNA was isolated (RNeasy Minikit; Qiagen Inc., Valencia, CA) and was further purified (RNeasy spin columns; Qiagen). The quantity and purity of each RNA sample was determined from the 260- and 280-nm absorbance, and its integrity was determined (2100 BioAnalyzer; Agilent Technologies Inc., Palo Alto, CA). Pooled RNA from two different corneal or conjunctival specimens (each one pair) was used for each replicate experiment. For both cornea and conjunctival tissues, there were one female and five male donors. This distribution merely resulted from the availability of donor tissue, as apportioned by the NDRI.

The pooled RNA was converted into cDNA with reverse transcriptase (SuperScript Choice; Invitrogen-Gibco, Bethesda, MD) and a modified oligodT primer (Affymetrix, Santa Clara,

CA). The purified cDNA was subjected to in vitro transcription to generate biotin-labeled cRNA (ENZO BioArray HighYield Kit; Affymetrix).

Microarray Hybridization and Data Processing

Appropriately fragmented biotin-labeled cRNA was hybridized to an oligonucleotide microarray (HG-U133A GeneChips; Affymetrix), according to the manufacture's protocol. Three separate experiments, each including one conjunctival and one corneal cRNA pool were performed. The HG-U133A array contains ~16, 000 unique GenBank accession numbers arranged in 22,283 probe sets (http://www.ncbi.nlm.nih.gov/Genbank; provided in the public domain by the National Center for Biotechnology Information, Bethesda, MD). Hybridized microarrays were stained with a streptavidin-phycoerythrin reagent, and fluorescence images were captured with a laser scanner (G2500A; Agilent).

Expression data were extracted from the fluorescence images (Microarray Analysis Suite, ver. 5.0 [MAS 5.0]; Affymetrix) to determine (1) the likelihood that the signal test result is significantly greater than the background signal, to determine whether the target transcript is present (P) or absent (A); and (2) a normalized signal intensity (SI) for each transcript. The data discussed in this publication have been deposited in the National Center for Biotechnology Information (NCBI) Gene Expression Omnibus (GEO, http://www.ncbi.nlm.nih.gov/geo/ provided in the public domain by the NCBI, Bethesda, MD) and are accessible through GEO Series accession number GSE5543. Annotation data were obtained from the Affymetrix Web site and by manual retrieval of selected transcripts from GenBank. Signal intensity values for all six individual data sets were subjected to unsupervised hierarchical clustering tests (conditional tree analysis) to assess the extent of global similarities and differences among the conjunctival and corneal replicates (GeneSpring; Silicon Genetics, Redwood City, CA).

To identify differentially expressed transcripts, the MAS 5.0-generated signal intensity triplicate data, without regard to present or absent status, was subjected to the local pooled error (LPE) statistical test, implemented in the R statistical programming language.[9] Transcripts included within the 1% false discovery rate level of the LPE test were considered to have a significantly different expression level between the two tissues. The MAS 5.0 signal intensity and P or A calls for all these transcripts were then transferred into a spreadsheet program (Excel; Microsoft, Redmond, WA) for further analysis. A transcript was considered present when it received a P call in at least two of the replicates and significant (S) when the mean SI for all three replicates exceeded 1% of the mean SI for the three β-actin transcripts represented in the microarray. The results were used to build conjunctival PS transcript (CnjPS) and corneal PS transcript (CoPS) spreadsheets. The CnjPS was then used to generate CnjPS/CoA, a transcript list containing all conjunctival PS transcripts that were completely absent from the cornea (designated A call in all three experiments) and CnjPS>1.5×CoP, a transcript list comprising all conjunctival PS transcripts not included in CnjPS/CoA for which the mean SI is at least 1.5 times as large as the respective corneal value. In an analogous manner, CoPS was used to build cornea-exclusive (CoPS/CnjA) and cornea-preferred (CoPS>1.5×CnjP) transcript lists. In the subsequent text, we alternatively refer to the sequences included in these lists as conjunctiva (or cornea-)-exclusive and conjunctiva (or cornea-)-preferred transcripts, respectively.

Analysis of Differential Gene Expression

Differentially expressed conjunctival and corneal transcripts were imported into the Expression Analysis Systematic Explorer software (EASE[10]; http://david.niaid.nih.gov/david/ease/htm/ provided in the public domain by the National Institute of Allergy and Infectious Diseases [NIAID]), to examine functional gene clusters of

the differentially expressed genes and/or to identify biological and molecular processes that are overrepresented in both tissues. EASE analysis with Bonferroni multiplicity correction probes each gene list against the corresponding population lists, and an EASE score is calculated for the likelihood of overrepresentation in the Gene Ontology Consortium annotation categories (GO biological process, GO cell component and GO molecular function; for sources of annotation, statistical methods, and EASE documentation, see the NIAID Web site).

Real-Time RT-PCR

Independent validation of relative expression levels by real-time PCR was performed with primer sets for all the connexin genes represented in the microarray. The RNA was obtained from epithelia mechanically scrapped from the corneal surface rather than from the Dispase release epithelial sheets and was treated with DNAase I (Qiagen) before its release from the purification columns (RNeasy Minikit; Qiagen), to eliminate possible contaminating genomic DNA, and was transcribed into cDNA (Omniscript reverse transcriptase; Qiagen). PCR reactions were performed with a SYBR green nucleic acid staining kit (Quantitect; Qiagen) in 384-well plates in a sequence-detection system (Prism 7900HT; Applied Biosystems [ABI], Foster City CA). For each primer pair, we used nine wells; three contained test cDNA, three contained a control sample in which the reverse transcriptase was omitted from the transcription reaction, and three contained human genomic DNA (Biochain, Hayward, CA). Products were analyzed by agarose (4%) gel chromatography. Relative amounts of the target genes in the corneal and conjunctival epithelia were then determined from the cycle thresholds according to the delta of delta C_t method using the average of the triplicate results. The following primer sets (forward/reverse) were used: Cx31, ccaacgtctgctacgacaactact/cacaggcctccgtgcttcttctt; Cx31.1, cccgacaccatgtgaagaaaa/tctcttgcctgcccctacct; Cx32, ggccgctccaatccac-ctt/gcggcgcagtatgtctttcag; Cx36, tcaaggaggtggaatgttatgtgt/tggcaggtcct-tgttacgaatct; Cx37, gagcactgatgggcacctatg/gctcgctggcacacaaaca; Cx40, gcctcccaacaaaacacagacaa/cataacgaacctggatgaaacctt; Cx43, cttttgatttc-cccgatgataacc/ggtgcactttctacagcacctttttt; Cx50, gaacccgaggtgggagagaa/ggcagcccttgctttgaca; Cx59, ttggggaaaatacaagttgaagaag/ataatcaggggca-gaagggagtc.

Cytohistochemistry

Freshly frozen human conjunctival (comprising predominantly of palpebral/forniceal conjunctival regions) and corneal cryosections (6–8 μm thick) were prepared for immunocytochemistry as previously described.[11–15] After fixation with ice-cold methanol at −20°C for 10 minutes, the tissue sections were incubated for 2 hours (RT) with monoclonal mouse antibodies against the following antigens: human secretory PLA_2 type II ($sPLA_2$-IIA; 1:100 dilution; Upstate Biotechnology, Lake Placid, NY), tyrosine-related protein-1 (TYRP-1; clone Ta99; 1:200 dilution; GeneTex, Inc., San Antonio, TX), and HLA class II (DP, DQ, DR; 1:200; Serotec, Raleigh, NC). Bound antibodies were stained by a 1-hour incubation with 1:500 diluted Alexa Fluor 488–conjugated goat anti-mouse IgG (Invitrogen-Molecular Probes Inc., Eugene, OR). The slides were rinsed three times with phosphate-buffered saline (PBS) and covered with antifade medium (Vectashield; Vector Laboratories, Burlingame, CA). Fluorescence was visualized on a fluorescence microscope (Axiophot2; Carl Zeiss Meditec, Inc., Thornwood, NY).

To identify melanocytes, we subjected the paraffin-embedded sections to Fontana-Masson silver stain (American Master Tech Sci., Lodi, CA). Briefly, the sections were incubated for 45 minutes at 60°C in ammoniacal silver solution, for 2 minutes in 5% sodium thiosulfate and for 5 minutes in nuclear fast red stain. To examine dihydronicotinamide adenine dinucleotide phosphate (NADPH) reductase activity,[16–17] cryosections were incubated for 2 to 4 hours at 37°C in 0.1 M phosphate buffer (pH 7.4) containing 2.5 mM NADPH

(Sigma-Aldrich, St. Louis, MO), 0.4 mM nitroblue tetrazolium (Sigma-Aldrich), and 10% dimethylsulfoxide. For control sections, NADPH was omitted from the incubation solution. The sections were rinsed in PBS, mounted in antifade medium (Vectashield; Vector Laboratories), and examined by light microscopy.

Results

RNA Quality

All RNA samples showed 260/280 nm absorption ratios in excess of 2.0. The RNA yields per single cornea and conjunctiva were approximately 6 and 20 μg, respectively. Based on cell counts independently obtained by trypsinization of epithelial sheets, these yields correspond to 4 to 6 pg RNA/cell, the typical RNA content of epithelial cells. Profiles (determined by Biochip; Agilent) were very similar in both tissues (Fig. 1). These profiles displayed a flat baseline, no significant tailing of the ribosomal RNA bands, and S18/S23 ratios of 1.5 to 1.8. RNA samples prepared from tissue that was released by scraping, instead of overnight Dispase incubation, showed poorer profiles (not shown), probably because of the presence of apoptotic or preapoptotic exfoliating surface cells, which are washed away during the Dispase incubation.

Microarray Analysis

Several empiric tests were used to evaluate the soundness of the raw data extracted (MAS 5.0; Affymetrix). The number of transcripts recognized by the software program as present in all three independent experiments was 9237 and 8905 for the conjunctiva and corneal epithelia, respectively. In addition, 1727 and 1633 further transcripts were identified in two of the experiments. Together, these transcripts account for approximately 50% (Cnj) and 48% (Co) of the total represented in the microarray. The number of P calls in each experiment and the median and average SIs (Table 1) or the distribution of twice present (PP) transcripts within the three experiments suggest no significant tissue bias in either of the replicates (not shown).

The microarray (HG-U133A; Affymetrix) contains three distinct probes for β-actin representing distinct sections of the gene. The similarity in average SIs for the spots representing the sequence segment closer to the polyA tail (bp 1201–1738) and the segment close to the starting codon (bp 50 –584), demonstrates that there was outstanding preservation of message length in the course of RNA isolation and generation of cRNA probes in experiments 1 and 2. There was some degradation, albeit of a similar degree in both tissues, in experiment 3 (Table 2). Because the probes for essentially all the transcripts in the Affymetrix microarray have been intentionally developed from the 3′ of the sequence, this degree of degradation is likely to have a minimal effect on our results. Similar results were obtained for the three GAPDH sequences present in the array (not shown). In addition, the similarity in the average SIs for conjunctival and corneal epithelia for this control gene indicates well-normalized SIs across the three experiments. Finally, conditional tree analyses of the whole transcript set or of the subsets of transcripts preferentially expressed in the Cnj and Co epithelia (Fig. 2) appropriately clustered the three conjunctival and corneal samples into two separate groups.

Identification of Differentially Expressed Genes

The differential analysis described in the Methods section resulted in the identification of a large number of genes that were uniquely or preferentially expressed in both epithelia. Since genes expressed at very low levels may not yield measurable levels of actual protein, we decided to limit the analysis to transcripts with expression higher than 1% of the highly expressed β-actin gene. The methodology outlined in the Methods section led to the

establishment of conjunctiva- and cornea-exclusive gene lists containing 93 and 339 transcripts, respectively, as well as 211 and 589 transcripts in the respective preferred gene lists. Genes included in the exclusive transcript sets were categorized according to relative SIs. For the preferred lists, to take into account both the level of expression and expression ratios as factors that would affect the phenotypic distinction between both tissues, we chose to use the product of the SI by the SI ratio (SI×R) as an index of significance.

The 25 genes with the highest SIs and SI×Rs, along with gene annotations are displayed in Tables 3 and 4, respectively. Note, that for many genes, the microarray chip (HG-U133A; Affymetrix) included two and even three transcript representations. In those instances in which a gene was represented in the array by more than one transcript set, only the transcript with the highest SI is displayed in Tables 3 and 4 (tissue ratios for these lower-SI transcripts were highly similar to those for the transcripts included in the tables). The top components of these lists include genes with high expression levels that have already been demonstrated, genes that are novel in these tissues, and genes of yet to be identified function. The full lists of the four exclusively or differentially expressed transcript sets have been included in the Appendix, online at http://www.iovs.org/cgi/content/full/48/5/2050/DC1. Updated functional GO annotations for each gene can be found at http://www.affymetrix.com/analysis/index.affx.

Pathway Identification by EASE/Gene Ontology Analyses

Exclusive and preferentially expressed conjunctival and corneal transcripts were amalgamated into conjunctival and corneal selective transcript lists containing 803 and 432 transcripts, respectively.

Affymetrix gene identifiers for both sets were imported into EASE software, to identify gene ontologies that are overexpressed in either tissue. This comparative analysis yielded several biological processes that were overrepresented in the corneal epithelium, albeit with only moderate to low significance scores (Table 5). The only noticeable group included activities related to cellular handling of heavy metals. In contrast, EASE analysis of selective conjunctival genes led to the identification of a large number of processes associated with very high levels of significance (EASE scores up to 10^{-28} and 10^{-24}, when subjected to Bonferroni adjustment). When the conjunctival statistically significant biological processes were organized into a GO ontology classification tree (http://www.geneontology.org), nearly all of the significantly overrepresented categories in the conjunctival epithelium coalesced within a narrow set of the physiological processes (Fig. 3) that includes two subcategories: genes related to responses to stimulus (stress, biotic, and external stimulus) and organismal physiological processes associated with immune mechanisms (humoral immune responses, including complement activation, antigen presentation, and processing). This level of statistical significance is probably attributable to the presence of a large number of HLA class II antigen mRNA within the conjunctival epithelium (Table 6; when more than one transcript is represented, only the highest SI representation has been included for each gene). Within the conjunctival epithelial layer, another category showing statistically significant overexpression related to melanin biosynthesis (Table 5).

Validation of Microarray Expression Levels

To validate the intensities obtained by the microarray study by real-time PCR, we chose a set of connexin transcripts represented in the microarray. The results for genomic DNA confirmed the similar effectiveness of all these primers against their respective targets (Table 7). Gel chromatography confirmed that, in each case, the SYBR green signal represented the generation of a single amplicon with the correct molecular size (not shown).

The comparison of the results from the Δ-Δ C_t and SI calculations demonstrate that the relative levels of expression and P/A status provided by the microarray accurately indicate the relative levels of expression reported by real-time PCR.

Histochemistry

The presence and localization of some of the most prominent conjunctiva-specific genes identified by the corneal– conjunctival comparison were examined by indirect immunofluorescence. Secretory PLA_2-IIA, the top gene in the Cnj epithelia-exclusive set was detectable at the protein level in conjunctival goblet cells and other superficial epithelial cells (Figs. 4A, 4B). Labeling occurred principally in granules accumulated in proximity to the plasma membrane that seem to be mobilized and excreted in Goblet cells undergoing active degranulation.

Cells expressing overly intense stain for HLA-class II antigen-presenting proteins (DR, DP, DQ) were intercalated throughout the suprabasal conjunctival epithelial cells (Fig. 4C). Neither of these proteins was expressed in the corneal epithelium (Figs. 4A, 4C, insets). Immunostaining for TYRP1 and the Fontana-Masson silver stain (Fig. 5) showed the abundant presence of melanocytes in the basal cell layer of the conjunctival epithelium. No staining was noted in the cornea (not shown).

Conversely, consistent with the existence of a highly expressed dehydrogenase reductase within the corneal preferred cohort (Table 4A), an enzymatic assay for NADH/NADPH reductase (diaphorase) activity revealed high reductase activity in the basal cells of the corneal epithelium (Fig. 6A), whereas activity throughout the conjunctival epithelium was minimal to nil (Fig. 6B).

Discussion

We have performed a microarray-based comparative global gene expression profiling (Affymetrix) of the two linings covering the ocular surface, the corneal and conjunctival epithelia. Given the embryologic and functionally related nature of these epithelial linings, the identification of genes and biological pathways that are specifically or preferentially expressed in either of these two tissues could selectively contribute to tissue phenotype and/or function. The use of SIs and PS/A calls (definitions for present and absent transcripts described in the Methods section), the LPE statistical approach, and a limitation of the analysis to substantially expressed transcripts led to the identification of 425 and 803 transcripts that were significantly overexpressed in the cornea and conjunctiva, respectively.

The most prominent global feature of the microarray data is the large excess of differentially expressed transcripts in the conjunctival set versus its corneal counterpart, and the high significance of EASE scores for multiple subcategories within the response to stimulus and organismal physiological processes (Fig. 3). This result probably reflects the multiphenotypic nature of the conjunctival epithelium.

Blood-derived intraepithelial antigen-presenting cells are numerous in this tissue (Fig. 4) and lymphocytes account for between 1% and 3% of the epithelial mass.[18,19] Consistent with this preponderance of intraepithelial leukocytes, the differential analysis identified multiple blood cell– exclusive cell markers (Tables 3B, 4B). Of the 29 MHC class II transcripts represented in the HG-U133A microarray, 20 were present in the differential conjunctival sets. Table 6 displays the genes represented by these transcripts. Notably, the expression levels for some of the MHC transcripts match the expression levels of housekeeping genes such as β-actin and GAPDH. MHC class II genes are expressed only in cells from the hematopoietic lineage. Thus, the results imply that the intraepithelial cells in

conjunctiva express class II genes at extraordinary levels. The very intense level of the immunostaining for HLA class II for DP, DQ, and/or DR subtypes (Fig. 4) is fully consistent with this conclusion. The presence of lymphocytes is reflected by the prominent location of the lymphocyte-specific protein 1 (LSP1) within the exclusive Cnj gene list (Table 3A). Likewise, the high concentration of melanocytes within the Cnj epithelial basal layer (Fig. 5) is reflected in the substantial representation of TYRP-1 and -2 (Tables 3, 4).

In contrast to conjunctival gene expression, the homogeneous cellular nature of the corneal epithelium generated minimal uncertainty as to the epithelial cell origin of transcripts that showed preferential expression in this tissue. EASE analysis indicated that the preferential expression of transcripts related to genes involved in the control of oxidative damage and heavy metal detoxification were the only biological processes that are more prominent in the corneal than in the conjunctival epithelia at a statistically significant level. The high levels of cornea-preferred genes of two well-known corneal proteins, aldolase dehydrogenase type 3AI and transketolase,[20,21] and of an NADH/NADPH reductase (diaphorase), known under the aliases of NQO1,[22] diaphorase 4, cytochrome b5 reductase, and dioxin-inducible menadione oxidoreductase, are likely to be the main contributors to the statistical significance of this EASE score (Tables 4A, 8). NQO1 has not been shown to be prominent in the cornea. Its function is to catalyze the two-electron reduction of quinones to hydroquinones, thereby preempting one-electron reduction of quinones by other reductases. The latter leads to the formation of detrimental reactive oxygen species. Overall, NQO1 could protect the cornea by directly scavenging free radicals or by allowing the rapid recovery of highly efficient free radical scavengers, such as ascorbate, to their active state.[23,24] The biological significance of NQO1 is also indicated by the fact that its absence leads to severe neurologic disability due to deficiencies in lipid and steroid metabolism that cause toxic accumulations in microsomal compartments.[25] Consistent with the NQO1 expression differences, our histochemical study of NADPH reductase indicates large differences in total oxiredox activity between corneal and conjunctival epithelia. Aldehyde dehydrogenase type 3A1 has recently been shown to be critical for corneal oxidative protection.[26] Considering that the gene expression level for diaphorase/NQO1 is similar to, and the Co/CNJ ratio is larger than, those for ALDH3A1, a detailed study of the role(s) played by this diaphorase in corneal biology appears to be highly warranted.

In addition to global gene expression analyses, it is also valuable to focus on the significance of individual transcripts (Table 8). The highest-expressing cornea-exclusive gene is testican 1. This large secreted multidomain proteoglycan has been shown to have strong inhibitory activity against cathepsin and activation of matrix metalloproteinases (MMPs).[27,28] The corneal epithelium expresses multiple MMPs and cathepsins, in particular, cathepsin L/V2,[29] which in itself shows a high corneal preference (Table 4A). Thus, it is intriguing to consider the possibility of a role for testican-1 in locally protecting the corneal epithelial cell surface membrane against the activity of its own proteolytic agents. The third gene in the cornea-exclusive list is a formin isoform. Formins are a conserved family of actin nucleators responsible for the assembly of diverse actin structures such as cytokinetic rings and filopodia. Formin binding to the barbed end of actin filaments increases filament flexibility and has been documented to cause critical modulation of cell adhesion and cell motility. The exclusive presence of a certain formin isoform in the corneal epithelium is likely to play a weighty role in the phenotypic difference of this tissue with that of its ocular surface counterpart. It will be interesting to assess formin's contribution to the rapid migration in corneal wound healing and response to physical pressure.[30] Another intriguing and unexpected corneal gene is cartilage acidic protein 1 (CRTAC1; Table 4A), a matrix component with high affinity for integrins. It is profusely expressed in cartilage, a mostly avascular tissue, but it is absent in most other organs and tissues examined, including brain, liver, and muscle.[31] Its corneal expression may indicate that its function is somehow related

to the avascular environs. Adiponectin, is another cornea-preferred, highly expressed gene. In a fashion similar to CRTAC1, it codes for a protein that until now has been believed to be specific for one cell type, the adipocyte.[32] Adiponectin is a secreted protein with multiple systemic functions including growth-promoting activity in epithelial cells.[33,34] If indeed, adiponectin is secreted by the corneal epithelium, it may function as part of the proliferation promoter autocrine loop. Other valuable corneal preferred genes to be considered for future investigations are chemokine CXCL14 (BRAK) and Dickkoft 3 (DKK3). CXCL14 plays a central role in monocyte attraction and their in situ conversion to Langerhans cells.[35] Thus, it could be important for the ontogeny of these immunosurveillance cells in the limbus. DKK proteins are involved in the regulation of the WNT-β-catenin cascade, which, in turn may control developmental cell fate[36] and the expression of connexin43, another highly expressed corneal preferred transcript (Table 4A). DKK2, which is not expressed in the mature human cornea (Table 9), has recently been found to be a critical component of corneal epithelial development in mouse.[37] Thus, it is possible that in humans, this role is performed by DKK3.

In the case of the conjunctival epithelium, the presence of substantial levels of infiltrated leukocytes and resident melanocytes implies that for most transcripts, confirmation of a bona fide epithelial origin will require specific spatial techniques such as in situ hybridization and/or immunohistochemistry. In the present study, we performed such a test for $sPLA_2$-IIA, a natural antimicrobial protein in tears[38,39] and a systemic proinflammatory mediator[40] that occupies the top position in the list of conjunctiva-expressed transcripts not expressed in the cornea (Table 3B). Immunohistology showed that the protein is abundantly expressed in the conjunctival Goblet cells. The stain displays spatial patterns and features suggestive of a secretory process (Fig. 4). To our knowledge, this is the first report of a nonmucinous secretion by mucin-rich cells anywhere in the body. Thus, the potential role(s) of this $sPLA_2$n in Goblet cell biology and secretory activity warrant further study. The more tenuous expression in other differentiated cells is consistent with the identification of high levels of gene and polypeptide expression of $sPLA_2$ class II, in a human conjunctival epithelial cell line that does not form mature Goblet cells.[41] Other very prominent conjunctival novel genes within the conjunctival lists that deserve future attention include lipocalin 2, an iron sequester protein that is part of tissue innate immunity[42]; insulin-like growth factor binding protein-3 (IGFBP3), a multifunctional soluble protein that regulates the potent mitogenic and antiapoptotic effects of IGF-I and -II and has been recently shown to have decreased expression in pterygium[43]; RARRES1, a retinoid receptor; trefoil factor 1, an estrogen-inducible protein; ceruloplasmin (Table 3B), and the Na-dependent phosphate transporter isoform NaPi-IIb (Table 4B). In the kidney proximal tubule and intestine, this transporter is localized at apical membranes, where it determines reabsorption or uptake of phosphate toward the circulation.[44,45] A similar role in the conjunctiva implies vigorous phosphate removal from the tears, which may be important in corneal protection; recent studies have shown that phosphate catalyzes corneal calcification.[46,47]

For some proteins (e.g., IGFBPs[48]) the two tissues displayed isoform expression differences. These secreted, high-affinity, IGF-binding proteins act as modulators of IGF bioavailability. Differential patterns of spatial and temporal expression in dynamic processes such a development and cellular transformation, indicate subtle differences in function. The corneal epithelium expresses high levels of the isoforms 6 and 7 (Table 4A). These isoforms are poorly expressed in the conjunctival epithelium which, conversely, shows a selectivity for isoform 3 (Table 4B).

Finally, in relation to keratins, the fundamental markers of epithelial phenotype, the microarray measurements yielded, as expected, high expression levels of the two cornea-specific keratins K3 and K12[49] (Table 10). In addition, consistent with its cornea-specific

classification, K3 was absent from the conjunctiva. K12, however, was expressed in this tissue at substantial levels. This result reflects the fact that patches of K12-expressing cells are intercalated within the conjunctival epithelium. As proposed by Kawasaki et al.,[50] the simplest interpretation of the patch pattern is the existence of a misdirected cell migration of corneal epithelial precursors from the limbus toward the conjunctiva. However, examination of other genes highly expressed in the cornea does not fit such a model. For instance, K3, testican-1, and ECM-1 transcripts well expressed in the cornea, are not found at all within the conjunctival set (Table 3A). In addition, the conjunctiva/cornea SI ratios for certain transcripts showing abundant corneal expression (e.g., cathepsin L2/V and NQO1 in Table 4A) are much lower than those for K12. Thus, none of those genes are substantially expressed within the K12-positive cells in the conjunctival cells. Therefore, the possibility that the cells in the K12-positive patches are not corneal cells but rather K12-expressing conjunctival cells requires attention. Other keratins also provide interesting distribution patterns. The simple epithelial keratin type 18 was moderately expressed by both tissues whereas K4, K13, K15, and K19 expression occurred at very high levels in the conjunctival domain only. These gene expression patterns in humans are generally coincident with reports of keratin protein expression in the ocular surface of rodents.[51] Finally, K19 has been mentioned occasionally as a potential limbal stem cell marker.[52] Given the conjunctival levels observed (Table 4B), it is unlikely that it plays such a function in the conjunctiva.

In summary, our microarray analysis of the embryologically related, yet phenotypically disparate corneal and conjunctival epithelia, allowed the identification of a large number of novel conjunctiva- and cornea-preferred transcripts for proteins that can have important roles in the ocular epithelial physiology of each of these tissues.

Acknowledgments

Supported by National Eye Institute Grants R01EY014878 and R03EY015132 (JMW).

The authors thank Tearina Chu, Director, Mount Sinai Microarray Facility, for helpful assistance.

References

1. Arcellana-Panlilio M, Robbins SM. Cutting-edge technology. I. Global gene expression profiling using DNA microarrays. Am J Physiol 2002;282:G397–G402.
2. Verducci JS, Melfi VF, Lin S, Wang Z, Roy S, Sen CK. Microarray analysis of gene expression: considerations in data mining and statistical treatment. Physiol Genomics 2006;25:355–363. [PubMed: 16554544]
3. Schena M, Shalon D, Davis RW, Brown PO. Quantitative monitoring of gene expression patterns with a complementary DNA microarray. Science 1995;270:467–470. [PubMed: 7569999]
4. Saghizadeh M, Kramerov AA, et al. Proteinase and growth factor alterations revealed by gene microarray analysis of human diabetic corneas. Invest Ophthalmol Vis Sci 2005;46:3604–3615. [PubMed: 16186340]
5. Sun CC, Su Pang JH, Cheng CY, et al. Interleukin-1 receptor antagonist (IL-1RA) prevents apoptosis in ex vivo expansion of human limbal epithelial cells cultivated on human amniotic membrane. Stem Cells 2006;24:2130–2139. [PubMed: 16741227]
6. Davis JA, Reed RR. Role of Olf-1 and Pax-6 transcription factors in neurodevelopment. J Neurosci 1996;16:5082–5094. [PubMed: 8756438]
7. Koroma BM, Yang JM, Sundin OH. The Pax-6 homeobox gene is expressed throughout the corneal and conjunctival epithelia. Invest Ophthalmol Vis Sci 1997;38:108–120. [PubMed: 9008636]
8. Nishina S, Kohsaka S, Yamaguchi Y, et al. PAX6 expression in the developing human eye. Br J Ophthalmol 1999;83:723–727. [PubMed: 10340984]

9. Jain N, Thatte J, Braciale T, Ley K, O'Connell M, Lee JK. Local-pooled-error test for identifying differentially expressed genes with a small number of replicated microarrays. Bioinformatics 2003;19:1945–1951. [PubMed: 14555628]
10. Hosack DA, Dennis G Jr, Sherman BT, Lane HC, Lempicki RA. Identifying biological themes within lists of genes with EASE. Genome Biol 2003;4:R70. [PubMed: 14519205]
11. Turner HC, Alvarez LJ, Candia OA, Bernstein AM. Characterization of serotonergic receptors in rabbit, porcine and human conjunctivae. Curr Eye Res 2003;27:205–215. [PubMed: 14562171]
12. Oen H, Cheng P, Turner HC, Alvarez LJ, Candia OA. Identification and localization of aquaporin 5 in the mammalian conjunctival epithelium. Exp Eye Res 2006;83:995–998. [PubMed: 16750192]
13. Turner HC, Bernstein A, Candia OA. Presence of CFTR in the conjunctival epithelium. Curr Eye Res 2002;24:182–187. [PubMed: 12221525]
14. Wolosin JM, Budak MT, Akinci MA. Ocular surface epithelial and stem cell development. Int J Dev Biol 2004;48:981–991. [PubMed: 15558489]
15. Budak MT, Alpdogan OS, Zhou M, Lavker RM, Akinci MA, Wolosin JM. Ocular surface epithelia contain ABCG2-dependent side population cells exhibiting features associated with stem cells. J Cell Sci 2005;118:1715–1724. [PubMed: 15811951]
16. Sandell JH. NADPH diaphorase cells in the mammalian inner retina. J Comp Neurol 1985;238:466–472. [PubMed: 4044926]
17. Sandell JH. NADPH diaphorase histochemistry in the macaque striate cortex. J Comp Neurol 1986;251:388–397. [PubMed: 3771835]
18. Gomes JA, Dua HS, Rizzo LV, Nishi M, Joseph A, Donoso LA. Ocular surface epithelium induces expression of human mucosal lymphocyte antigen (HML-1) on peripheral blood lymphocytes. Br J Ophthalmol 2004;88:280–285. [PubMed: 14736792]
19. Gomes JA, Jindal VK, Gormley PD, Dua HS. Phenotypic analysis of resident lymphoid cells in the conjunctiva and adnexal tissues of rat. Exp Eye Res 1997;64:991–997. [PubMed: 9301480]
20. Pappa A, Estey T, Manzer R, Brown D, Vasiliou V. Human aldehyde dehydrogenase 3A1 (ALDH3A1): biochemical characterization and immunohistochemical localization in the cornea. Biochem J 2003;376:615–623. [PubMed: 12943535]
21. Sax CM, Salamon C, Kays WT, et al. Transketolase is a major protein in the mouse cornea. J Biol Chem 1996;271:33568–33574. [PubMed: 8969223]
22. Vasiliou V, Ross D, Nebert DW. Update of the NAD(P)H:quinone oxidoreductase (NQO) gene family. Hum Genomics 2006;2:329–335. [PubMed: 16595077]
23. Gomez-Diaz C, Rodriguez-Aguilera JC, Barroso MP, et al. Antioxidant ascorbate is stabilized by NADH-coenzyme Q10 reductase in the plasma membrane. J Bioenerg Biomembr 1997;29:251–257. [PubMed: 9298710]
24. Kurian JR, Bajad SU, Miller JL, Chin NA, Trepanier LA. NADH cytochrome b5 reductase and cytochrome b5 catalyze the microsomal reduction of xenobiotic hydroxylamines and amidoximes in humans. J Pharmacol Exp Ther 2004;311:1171–1178. [PubMed: 15302896]
25. Jaffe ER. Enzymopenic hereditary methemoglobinemia: a clinical/biochemical classification. Blood Cells 1986;12:81–90. [PubMed: 3539237]
26. Estey T, Piatigorsky J, Lassen N, Vasiliou V. ALDH3A1: a corneal crystallin with diverse functions. Exp Eye Res 2007;84:3–12. [PubMed: 16797007]
27. Edgell CJ, BaSalamah MA, Marr HS. Testican-1: a differentially expressed proteoglycan with protease inhibiting activities. Int Rev Cytol 2004;236:101–122. [PubMed: 15261737]
28. Hausser HJ, Decking R, Brenner RE. Testican-1, an inhibitor of pro-MMP-2 activation, is expressed in cartilage. Osteoarthritis Cartilage 2004;12:870–877. [PubMed: 15501402]
29. Kenney MC, Chwa M, Atilano SR, et al. Increased levels of catalase and cathepsin V/L2 but decreased TIMP-1 in keratoconus corneas: evidence that oxidative stress plays a role in this disorder. Invest Ophthalmol Vis Sci 2005;46:823–832. [PubMed: 15728537]
30. Faix J, Grosse R. Staying in shape with formins. Dev Cell 2006;10:693–706. [PubMed: 16740473]

31. Zhao GQ, Zhou X, Eberspaecher H, Solursh M, de Crombrugghe B. Cartilage homeoprotein 1, a homeoprotein selectively expressed in chondrocytes. Proc Natl Acad Sci USA 1993;90:8633–8637. [PubMed: 7690966]
32. Scherer PE, Williams S, Fogliano M, Baldini G, Lodish HF. A novel serum protein similar to C1q, produced exclusively in adipocytes. J Biol Chem 1995;270:26746–26749. [PubMed: 7592907]
33. Mendez-Sanchez N, Chavez-Tapia NC, Zamora-Valdes D, Uribe M. Adiponectin, structure, function and pathophysiological implications in non-alcoholic fatty liver disease. Mini Rev Med Chem 2006;6:651–656. [PubMed: 16787375]
34. Ogunwobi OO, Beales IL. Adiponectin stimulates proliferation and cytokine secretion in colonic epithelial cells. Regul Pept 2006;134:105–113. [PubMed: 16529829]
35. Schaerli P, Willimann K, Ebert LM, Walz A, Moser B. Cutaneous CXCL14 targets blood precursors to epidermal niches for Langerhans cell differentiation. Immunity 2005;23:331–342. [PubMed: 16169505]
36. van der Horst G, van der Werf SM, Farih-Sips H, van Bezooijen RL, Lowik CW, Karperien M. Downregulation of Wnt signaling by increased expression of Dickkopf-1 and -2 is a prerequisite for late-stage osteoblast differentiation of KS483 cells. J Bone Miner Res 2005;20:1867–1877. [PubMed: 16160745]
37. Mukhopadhyay M, Gorivodsky M, Shtrom S, et al. Dkk2 plays an essential role in the corneal fate of the ocular surface epithelium. Development 2006;133:2149–2154. [PubMed: 16672341]
38. Buckland AG, Wilton DC. The antibacterial properties of secreted phospholipases A(2). Biochim Biophys Acta 2000;1488:71–82. [PubMed: 11080678]
39. Moreau JM, Girgis DO, Hume EB, Dajcs JJ, Austin MS, O'Callaghan RJ. Phospholipase A(2) in rabbit tears: a host defense against Staphylococcus aureus. Invest Ophthalmol Vis Sci 2001;42:2347–2354. [PubMed: 11527949]
40. Touqui L, Wu YZ. Interaction of secreted phospholipase A2 and pulmonary surfactant and its pathophysiological relevance in acute respiratory distress syndrome. Acta Pharmacol Sin 2003;24:1292–1296. [PubMed: 14653960]
41. Hori Y, Spurr-Michaud SJ, Russo CL, Argueso P, Gipson IK. Effect of retinoic acid on gene expression in human conjunctival epithelium: secretory phospholipase A2 mediates retinoic acid induction of MUC16. Invest Ophthalmol Vis Sci 2005;46:4050–4061. [PubMed: 16249480]
42. Berger T, Togawa A, Duncan GS, et al. Lipocalin 2-deficient mice exhibit increased sensitivity to Escherichia coli infection but not to ischemia-reperfusion injury. Proc Natl Acad Sci USA 2006;103:1834–1839. [PubMed: 16446425]
43. Wong YW, Chew J, Yang H, Tan DT, Beuerman R. Expression of insulin-like growth factor binding protein-3 in pterygium tissue. Br J Ophthalmol 2006;90:769–772. [PubMed: 16488932]
44. Xu L, Dixit MP, Chen R, et al. Effects of angiotensin II on NaPi-IIa co-transporter expression and activity in rat renal cortex. Biochim Biophys Acta 2004;15(1667):114–121. [PubMed: 15581846]
45. Radanovic T, Wagner CA, Murer H, Biber J. Regulation of intestinal phosphate transport. I. Segmental expression and adaptation to low-P(i) diet of the type IIb Na(+)-P(i) cotransporter in mouse small intestine. Am J Physiol 2005;288:G496–G500.
46. Schrage NF, Schlossmacher B, Aschenberner W, et al. Phosphate buffer in alkali eye burns as an inducer of experimental corneal calcification. Burns 2001;27:459–464. [PubMed: 11451598]
47. Bernauer W, Thiel MA, Langenauer UM, Rentsch KM. Phosphate concentration in artificial tears. Graefes Arch Clin Exp Ophthalmol 2006;244:1010–1014. [PubMed: 16418839]
48. Hwa V, Oh Y, Rosenfeld RG. The insulin-like growth factor-binding protein (IGFBP) superfamily. Endocr Rev 1999;20:761–787. [PubMed: 10605625]
49. Kinoshita S, Adachi W, Sotozono C, et al. Characteristics of the human ocular surface epithelium. Prog Retin Eye Res 2001;20:639–673. [PubMed: 11470454]
50. Kawasaki S, Tanioka H, Yamasaki K, Yokoi N, Komuro A, Kinoshita S. Clusters of corneal epithelial cells reside ectopically in human conjunctival epithelium. Invest Ophthalmol Vis Sci 2006;47:1359–1367. [PubMed: 16565369]
51. Kasper M. Patterns of cytokeratins and vimentin in guinea pig and mouse eye tissue: evidence for regional variations in intermediate filament expression in limbal epithelium. Acta Histochem 1992;93:319–332. [PubMed: 1382351]

52. Schlotzer-Schrehardt U, Kruse FE. Identification and characterization of limbal stem cells. Exp Eye Res 2005;81:247–264. [PubMed: 16051216]

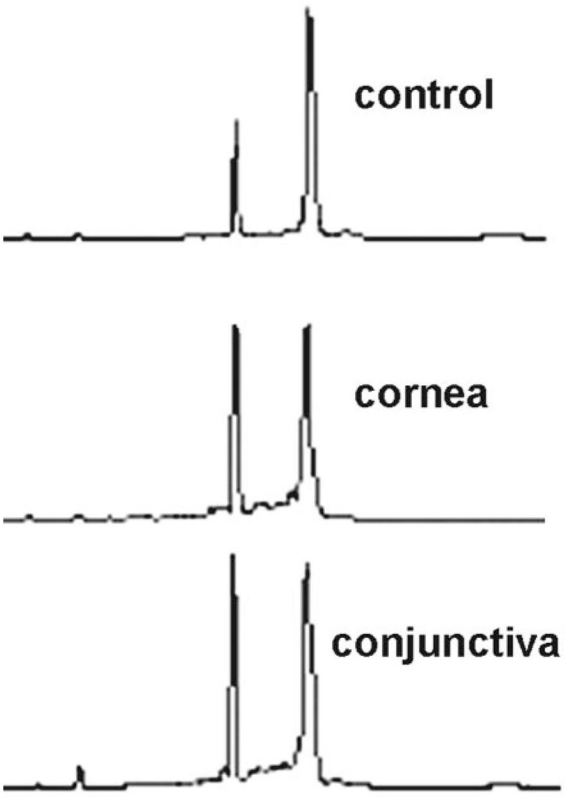

Figure 1.
Biochip profiles (Agilent, Palo Alto, CA) of total RNA isolated from Dispase-released corneal and conjunctival epithelia.

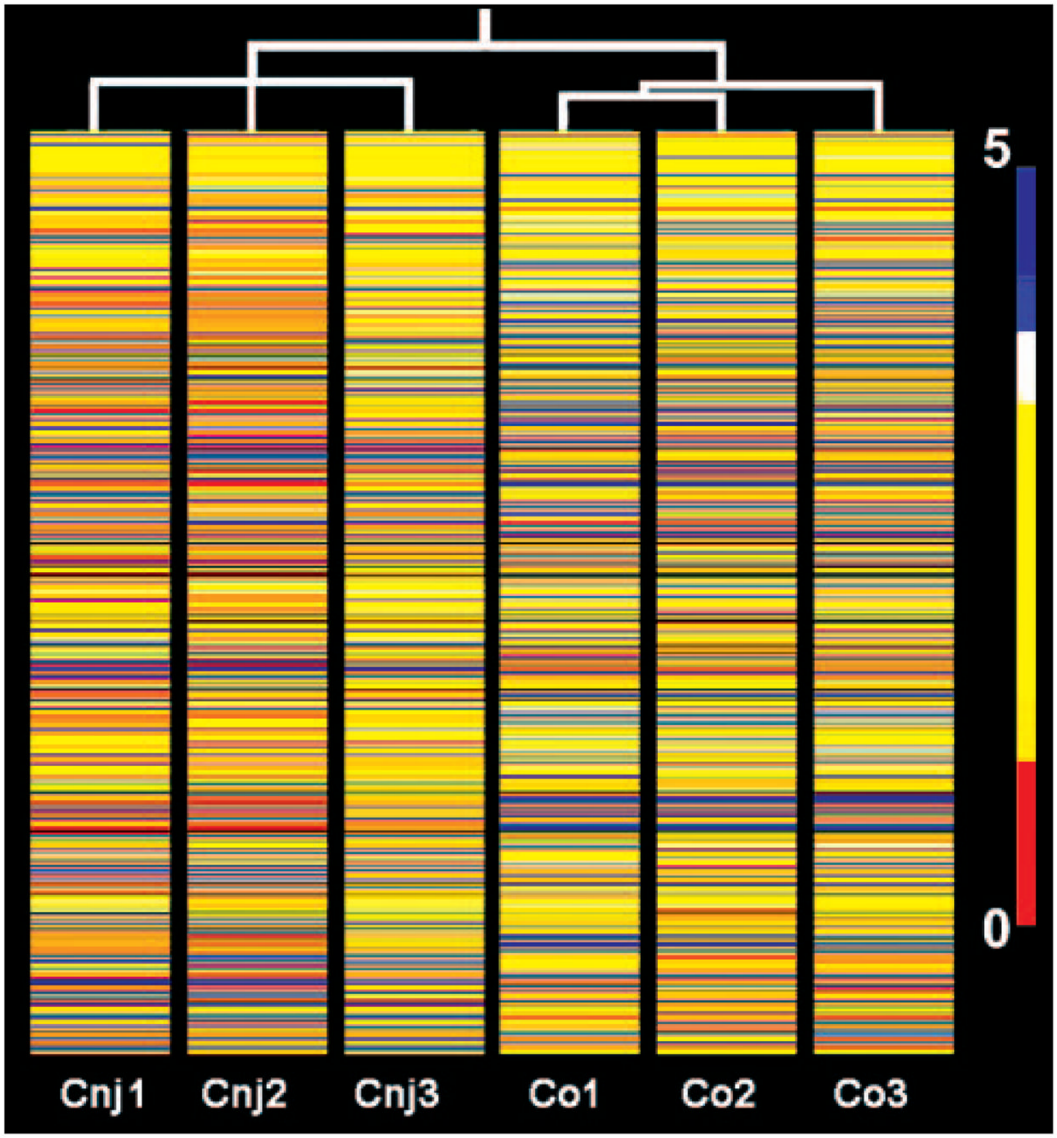

Figure 2.

Heat map for unsupervised hierarchical sample clustering of corneal and conjunctival transcripts with significant expression. Whole transcript sets for three conjunctival (Cnj1-3) and three corneal (Co1-3) samples were clustered by the unsupervised hierarchical sample method (Pearson correlation similarity measurement) to generate a sample tree (*vertical lines*). Note that the process has correctly clustered the two cell types. The 1228 statistically different transcripts (803 for the Cnj and 425 for the Co samples) are shown as individual horizontal color-coded lines within this sample tree, where color represents relative expression level in a base 10 logarithmic scale. The color code is shown in the *right* side bar.

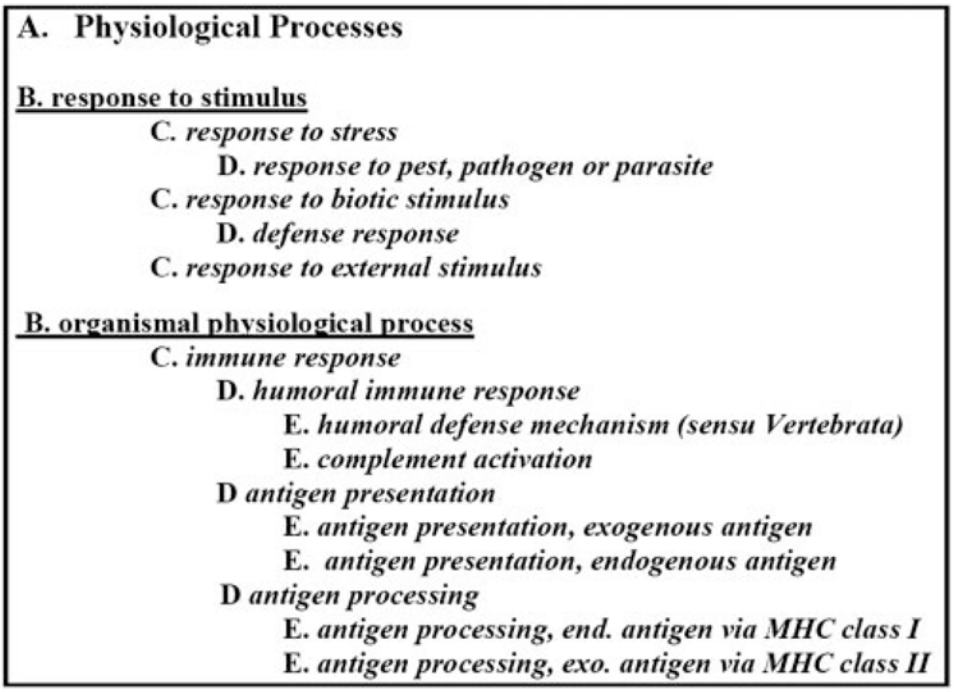

Figure 3.
Hierarchical tree of GO ontology processes significantly overrepresented in the Cnj epithelium.

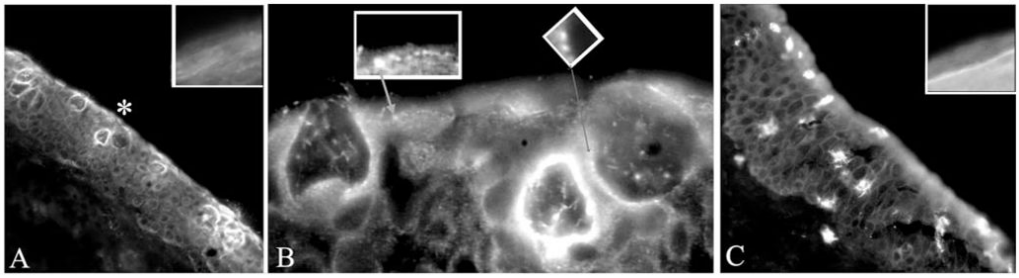

Figure 4.

Immunolocalization of $sPLA_2$-IIA and HLA-II antigen presenting cells in freshly isolated human conjunctival epithelium. Cryosections (5–8 mm thick) fixed in ice-cold methanol were probed with anti-human sPLA2-IIA and HLA-II antibodies. (**A**) Low magnification demonstrates that the sPLA2-IIA protein predominantly labeled to immature and mature Goblet cells. (**B**) Higher magnification of the *asterisk*-marked area reveals that the sPLA2-IIA protein was distributed in both Goblet and non-Goblet cells in vesicular granules structures within or in proximity to the plasma membrane. In surface goblet cells undergoing degranulation, numerous vesicle profiles were observed migrating toward the cell secretory pit, whereas vesicular density at the membrane wall appeared markedly reduced. Cells containing very high levels of HLA-II antigen distributed between the Cnj epithelial stratum (**C**). (**A**, **C**, *insets*) Results for the cornea.

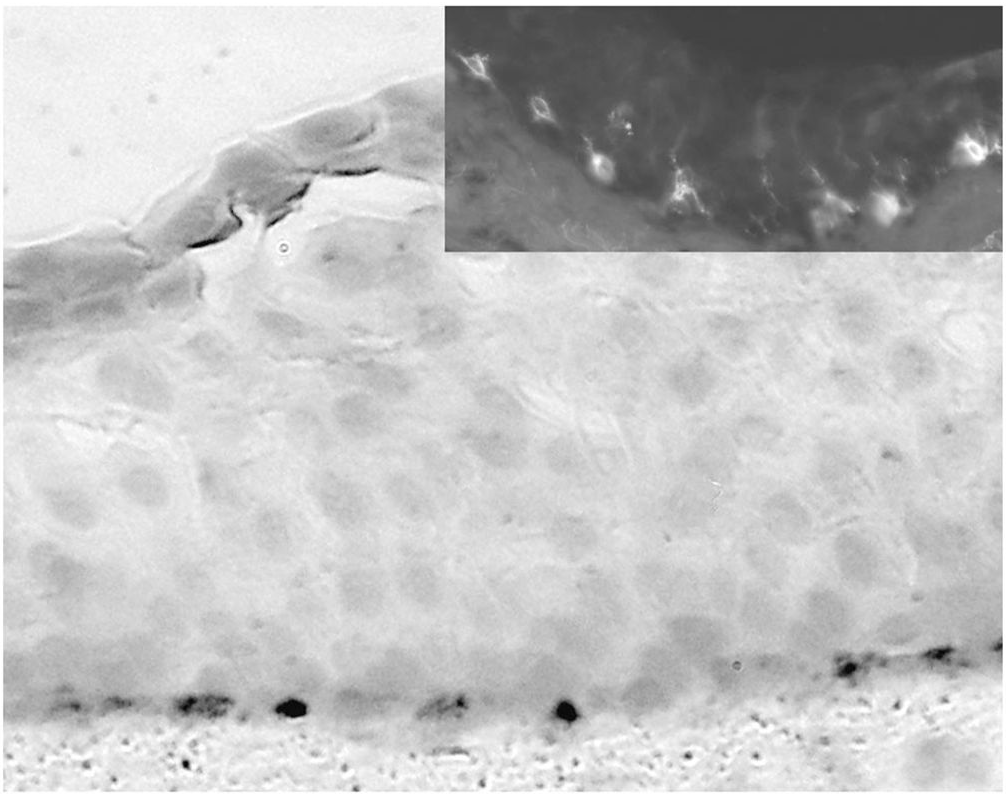

Figure 5.
Fontana-Mason stain of the mucocutaneous zone of human conjunctiva and immunostain for TYRP1 in the palpebral conjunctiva (*inset*). Note the high frequency of stained cells in the basal layer in both cases.

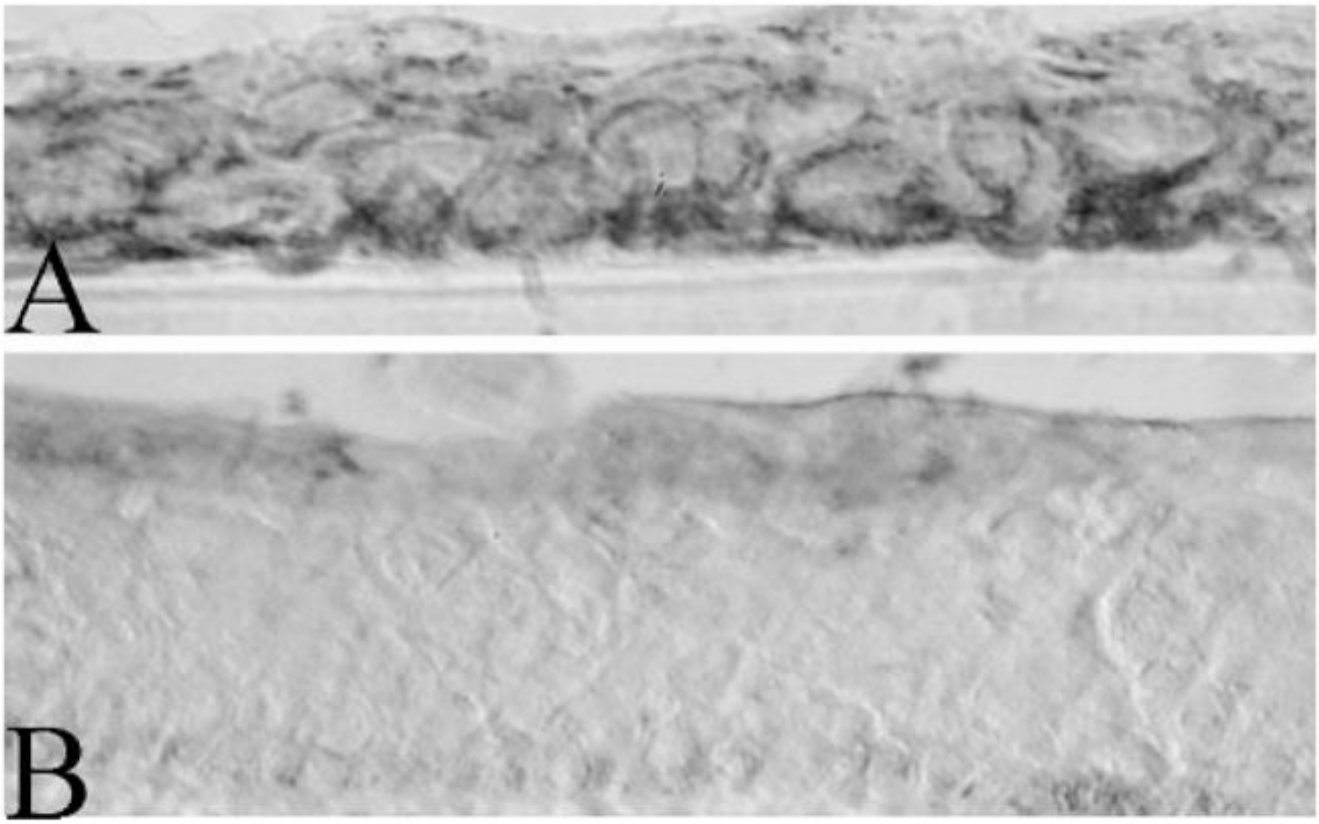

Figure 6.
Distribution of NADPH reductase activity in the conjunctival and corneal epithelium. Activity was found in the basal stratum of the corneal epithelium (**A**) but not in the conjunctival epithelium (**B**).

Table 1

Number of P Calls and Median and Mean SIs and Distribution of Present (P), Marginal, (M) and Absent (A) Calls in Each of the Three Experiments

		Experiment				
	Tissue	**1**	**2**	**3**	**Mean**	**SD**
P calls (*n*)	Conjunctiva	11,593	10,377	10,901	10,957	610
	Cornea	10,125	11,101	10,687	10637	490
SI Median/Mean	Conjunctiva	57.1/234	61.0/238	53.6/244	57.2/239	3.7/5
	Cornea	57.7/242	56.7/226	53.4/244	55.9/238	2.2/10

Table 2

SIs for the Three β-Actin Sequence Zones Represented in the HG U133A Microarray in the Two Epithelia in the Three Experiments

	Conjunctival Epithelium				Corneal Epithelium			
β-Actin Sequence* (bp Segment)	**Exp. 1**	**Exp. 2**	**Exp. 3**	**Mean**	**Exp. 1**	**Exp. 2**	**Exp. 3**	**Mean**
50–584 (5′ end)	4911	3998	1422	3444	3420	4992	1300	3237
645–1173 (center)	5699	5218	3656	4858	4569	7009	3302	4960
1201–1738 (3′ end)	5014	5037	5145	5066	4331	4434	4476	4414
Ratio 3′/5′	1.02	1.26	3.62	1.47	1.27	0.89	3.44	1.36
Averages ± SD	5208	4751	3408	4456 936	4107	5478	3026	4204 1229

*GenBank Accession X00351.1.

Invest Ophthalmol Vis Sci. Author manuscript; available in PMC 2010 July 26.

Table 3

Transcripts Exhibiting the Highest Expression in the Co- and Cnj-Exclusive Sets

A. CoPS/CnjA Set

Affymetrix	GB Accession	SI	Gene	Symbol
202363_at	AF231124.1	1,136.5	Testican1/sparc/osteonectin	*SPOCK1*
209365_s_at	U65932.1	1,106.9	Extracellular matrix protein 1	*ECM1*
218980_at	NM_025135.1	884.2	Formin homology 2, dcm 3	*FHOD3*
208789_at	BC004295.1	780.6	Polymerase 1 and transcript release factor	*PTRF*
201481_s_at	NM_002862.1	544.2	Phosphorylase, glycogen; brain	*PYGB*
213236_at	AK025495.1	528.3	Sam and sh3, dmc 1	*SASH1*
201108_s_at	BF055462	468.6	Thrombospondin 1	*THBS1*
201465_s_at	BC002646.1	417.3	v-Jun avian sarcoma virus 17 oncogene homolog	*JUN*
206423_at	NM_021146.1	414.8	Angiopoietin-like 7	*ANGPTL7*
205397_x_at	U76622.1	410.4	Smad, mothers against dpp, h 3	*SMAD3*
207114_at	NM_025261.1	383.4	Lymphocyte antigen 6 complex, locus g6c	*LY6G6C*
220291_at	NM_017711.1	379.8	Glycerophosphodiester phosphodiesterase, dmc 2	*GDPD2*
206207_at	NM_001828.3	341.7	Charot-leyden crystal protein	*CLC*
214961_at	A1818409	311.8	KIAA0774	*KIAA0774*
209469_at	BF939489	292.7	Glycoprotein, m 6a	*GPM6A*
203980_at	NM_001442.1	286.5	Adipocyte fatty acid binding protein 4	*FABP4*
213652_at	AU152579	286.1	Proprotein convertase subtilisin/kexin, t 5	*PCSK5*
216080_s_at	AC004770	276.3	Fatty acid desaturase 3	*FADS3*
221291_at	NM_025217.1	265.1	U116-binding protein 2	*ULBP2*
214680_at	BF674712	264.0	Neurotrophic tyrosine kinase, receptor, t 2	*NTRK2*
216603_at	AL365343.2	262.8	Carrier family 7/cationic aa transporter, m 8	*SLC7A8*
204726_at	NM_001257.1	258.1	Cadherin 13, h-cadherin (heart)	*CDH13*
206706_at	NM_002527.2	241.3	Neurotrophin 3	*NTF3*
211891_s_at	AB042199.1	233.1	Rho guanine nucleotide exchange factor (gef) 4	*ARHGEF4*
202729_s_at	NM_000627.1	230.6	Latent tgf beta binding protein 1	*LTBP1*

B. CnjPS/CoA Set

Affymetrix	GB Accession	SI	Gene	Symbol
203649_s_at	NM_000300.1	6,529.8	Phospholipase A2, group IIA (platelets, synovial)	*PLA2G2A*
221872_at	A1669229	4,089.4	Retinoic acid receptor responder (tazarotene induced) 1	*RARRES1*
213611_at	BF726531	2,280.4	Aquaporin 5	*AQP5*
205009_at	NM_003225.1	1,892.4	Trefoil factor 1 (estrogen-inducible sequence)	*TFF1*
204846_at	NM_000096.1	1,724.8	Ceruloplasmin (ferroxidase)	*CP*
218990_s_at	NM_005416.1	1,298.0	Small proline-rich protein 3	*SPRR3*
204213_at	NM_002644.1	1,044.4	Polymeric immunoglobulin receptor	*PIGR*
214063_s_at	AI073407	838.5	Transferrin	*TF*
209278_s_at	L27624.1	715.9	Tissue factor pathway inhibitor 2	*TFP12*
212671_s_at	BG397856	683.4	Major histocompatibility complex, class II, DQ alpha 1*	*HLA-DQA1*
205044_at	NM_014211.1	679.5	Gamma-aminobutyric acid (GABA) A receptor, p1	*GABRP*

A. CoPS/CnjA Set

Affymetrix	GB Accession	SI	Gene	Symbol
205338_s_at	NM_001922.2	658.9	Dopachrome tautomerase (tyrp 2)†	*DCT*
217059_at	L13283.1	638.4	Mucin 7, secreted	*MUC7*
210096_at	J02871.1	634.0	Cytochrome P450, family 4, subfamily B, polypeptide 1	*CYP4B1*
204623_at	NM_003226.1	608.7	Trefoil factor 3 (intestinal)	*TFF3*
219630_at	NM_005764.1	571.2	PDZK1 interacting protein 1	*PDZK1IP1*
214566_at	NM_012390.1	532.8	Submaxillary gland androgen regulated protein 3 h A	*SMR3A*
203523_at	NM_002339.1	516.6	Lymphocyte-specific protein 1, isoform 1*	*LSP1*
211656_x_at	M32577.1	453.7	Major histocompatibility complex, class II, DQ beta 1*	*HLA-DQB1*
209498_at	X16354.1	449.7	Carcinoembryonic antigen-related cell adhesion, m 1	*CEACAM1*
206509_at	NM_002652.1	428.5	Prolactin-induced protein	*PIP*
209488_s_at	D84109.1	428.2	RNA binding protein with multiple splicing	*RBPMS*
215388_s_at	X56210.1	412.5	Complement factor H -related protein 1	*CFH*
204897_at	AA89756	407.3	Prostaglandin E receptor 4 (subtype EP4)	*PTGER4*
221667_s_at	AF133207.1	397.1	Heat shock 22kDa protein 8	*HSPB8*

Affymetrix, Santa Clara, CA. GB, GenBank; dmc, domain containing; m, member; h, homologue; t, type.

*Leucocyte-associated gene.

†Melanocyte-associated gene.

Table 4

Transcripts Displaying the Highest SI×R Times SI in the Co- and Cnj-Preferred Sets

A. CojPS > 1.5 CoCNJ Transcripts Displaying the Highest CoPS/Cnj SI Ratio Times Co SIs

Affymetrix	Accession	SI	Ratio	SI × R × 10^{-3}	Gene	Symbol
221204_s_at	NM_018058.1	5,275.2	35.5	187	Cartilage acidic protein 1	*CRTAC1*
210074_at	AF070448.1	6,529.5	24.9	163	Cathepsin L2/V	*CTSL2*
201467_s_at	AI039874	4,366.9	26.5	116	NAD(P)H dehydrogenase, quinone 1	*NQO1*
207811_at	NM_000223.1	10,029.9	9.8	98	Keratin 12 (Meesmann corneal dystrophy)	*KRT12*
214247_s_at	AU148057	2,311.4	36.2	84	Dickkopf homolog 3	*DKK3*
208699_x_at	BF696840	6,952.8	10.7	74	Transketolase (Wernicke-Korsakoff synd.)	*TKT*
201667_at	NM_000165.2	4,573.3	15.5	71	Connexin 43	*GJAI*
220267_at	NM_019016.1	3,349.7	18.7	63	Keratin 24	*KRT24*
203571_s_at	NM_006829.1	9,858.8	4.6	46	Adiponectin/adipose specific collagen-like	*APM1*
218002_s_at	NM_004887.1	5,828.2	7.8	46	Chemokine (C-X-C motif) ligand 14	*CXCL14*
204777_s_at	NM_002371.2	3,985.3	9.3	37	Mal, T-cell differentiation protein	*MAL*
205623_at	NM_000691.1	11,199.8	3.3	35	Aldehyde dehydrogenase 3 family, m A1	*ALDH3A1*
219736_at	NM_018700.1	782.0	38.8	30	Tripartite motif-containing 36	*TRIM36*
206642_at	NM_001942.1	2,237.5	11.1	25	Desmoglein 1	*DSG1*
217294_s_at	U88968.1	8,135.6	3.0	24	Enolase 1, (alpha)	*ENO1*
200748_s_at	NM_002032.1	10,141.7	2.4	24	Ferritin, heavy polypeptide 1	*FTH1*
203851_at	NM_002178.1	4,844.0	4.7	23	Insulin-like growth factor binding protein 6	*IGFBP6*
221795_at	AI346341	986.4	22.6	22	Neurotrophic tyrosine kinase, receptor, type 2	*NTRK2*
211628_x_at	J04755.1	10,458.9	2.1	22	Ferritin, heavy polypeptide pseudogene 1	*FTHP1*
204753_s_at	A1810712	1,281.2	17.1	22	Hepatic leukemia factor	*HLF*
204326_x_at	NM_002450.1	6,870.3	3.2	22	Metallothionein IX	*MT1X*
212543_at	U83115.1	3,913.5	4.7	18	Absent in melanoma 1	*AIM1*
201162_at	NM_001553.1	2,596.0	6.6	17	Insulin-like growth factor binding protein 7	*IGFBP7*
212224_at	NM_000689.1	5,397.7	3.0	16	Aldehyde dehydrogenase 1 family, m A1	*ALDHIA1*
218309_at	NM_018584.1	2,598.2	5.8	15	Calcium/calmodulin PK II inhibitor 1	*CAMK2N1*
203781_at	NM_004891.1	14,039	3.38	14	Mitochondrial ribosomal protein L33	*MRPL33*
203074_at	NM_001630.1	13,457	2.46	13	Annexin 8	*ANXA8*

A. CojPS > 1.5 CoCNJ Transcripts Displaying the Highest CoPS/Cnj SI Ratio Times Co SIs

Affymetrix	Accession	SI	Ratio	SI × R × 10^{-3}	Gene	Symbol
212185_x_at	NM_005953.1	13,433	2.42	13	Metallothionein 2A	*MT2A*
200872_at	NM_002966.1	12,788	2.68	13	S100 calcium-bind protein A10	*S100A10*
219093_at	NM_017933.1	12,397	20.63	12	Hypothetical protein FLJ20701	*FLJ20701*
211538_s_at	U56725.1	12,193	13.85	12	Heat shock protein 70	*HSPA2*

B. The CnjPS > 1.5 CoP Transcripts Displaying the Highest Cnj/Co SI Ratio Times Cnj SIs

Affymetrix	GB Accession	SI	Ratio	SI × R × 10^{-3}	Gene	Symbol
212531_at	NM_005564.1	7,589.4	134.7	1022	Lipocalin 2 (oncogene 24p3)	*LCN2*
210095_s_at	M31159.1	5,671.6	103.9	589	Insulin-like growth factor binding protein 3	*IGFBP3*
207935_s_at	NM_002274.1	8,808.5	62.5	551	Keratin 13	*KRT13*
203021_at	NM_003064.1	7,415.1	53.0	393	Secretory leukocyte protease inhibitor	*SLP1*
201650_at	NM_002276.1	5,965.1	43.4	259	Keratin 19	*KRT19*
203535_at	NM_002965.2	7,321.1	35.2	258	S100 calcium-binding protein A9	*S100A9*
201884_at	NM_004363.1	2,535.4	69.4	176	Carcinoembryonic antigen-related cell adhesion, m 5	*CEACAM5*
211657_at	M18728.1	3,308.9	52.3	173	Carcinoembryonic antigen-related cell adhesion, m 6	*CEACAM6*
209619_at	K01144.1	4,577.2	35.5	163	CD74, binds MHC class II protein invariant chain*	*CD74*
210982_s_at	M60333.1	2,738.9	59.2	162	MHC class II HLA-DRA*	*HLA-DRA*
206199_at	NM_006890.1	2,554.3	59.1	151	Carcinoembryonic antigen-related cell adhesion m 7	*CEACAM7*
204351_at	NM_005980.1	2,607.1	55.2	144	S100 calcium-binding protein P	*S100P*
202917_s_at	NM_002964.2	9,208.7	14.0	129	S100 calcium-binding protein A8 (calgranulin A)	*S100A8*
209312_x_at	U65585.1	4,072.5	30.2	123	MHC class II, DR beta 4*	*HLA-DRB4*
213240_s_at	X07695.1	7,173.0	10	71	Keratin 4	*KTR4*
203963_at	NM_001218.2	1,394.0	43.1	60	Carbonic anhydrase XII	*CA12*
205694_at	NM_000550.1	1,581.9	35.7	56	Tyrosinase-related protein 1†	*TYRP1*
209140_x_at	L42024.1	8,632.4	6.2	53	MHC HLA-B39*	*HLA-B39*
204124_at	AF146796.1	1,370.3	37.7	52	Sodium dependent phosphate transporter isoform IIb	*NaPi-IIb*
203892_at	NM_006103.1	2,186.1	23.4	51	WAP four-disulfide core domain 2	*WFDC2*
213568_at	A1811298	1,112.7	40.0	44	Odd-skipped related 2 (Drosophila)	*OSR2*
211990_at	M27487.1	2,043.1	21.2	43	MHC class II DPw3-alpha-1 chain*	*HLA-DPA1*

A. CojPS > 1.5 CoCNJ Transcripts Displaying the Highest CoPS/Cnj SI Ratio Times Co SIs

Affymetrix	Accession	SI	Ratio	SI × R × 10^{-3}	Gene	Symbol
211911_x_at	L07950.1	6,604.4	6.4	43	MHC class I, B	*HLA-B*
214459_x_at	M12679.1	7,628.3	5.4	41	MHC class I, C	*HLA-C*
211429_s_at	AF119873.1	1,287.3	31	40	Serpin peptidase inhibitor (alpha-1 antiproteinase) m1	*SERPINA1*
214022_s_at	AA749101	1,892.7	20.7	38	Interferon induced transmembrane protein 1 (9–27)	*IFITM1*
213693_s_at	A1610869	1,091.7	35.1	38	Mucin I, transmembrane	*MUC1*
204363_at	NM_001993.2	2,332.7	15.5	36	Thromboplastin coagulation factor III	*F3*
204734_at	NM_002275.1	3,422.0	10.0	34	Keratin 15	*KTR15*
202357_s_at	gb:NM_001710.1	1,455.8	23.1	34	Complement factor B	*CFB*

Affymetrix, Santa Clara, CA. GB, GenBank.

*Leucocyte associated gene.

†Melanocyte associated gene.

Table 5

Biological Processes Overrepresented within the Differentially Expressed Transcripts in the Conjunctival and Corneal Epithelium

	Conjunctival Epithelium	
Corneal Epithelium $10^{-3} – 5 \times 10^{-2}$*	**$10^{-28} – 10^{-5}$***	**$10^{-5} – 10^{-2}$***
Cell adhesion	Response to biotic stimulus	Response to wounding
Transition metal ion homeostasis	Immune response	Inflammatory response
Copper ion homeostasis	Defense response	Innate immune response
Epidermal differentiation	Response to external stimulus	Complement activation, classic pathway
Heavy metal sensitivity/resistance	Antigen processing	
Posttranslational membrane targeting	Antigen presentation	Nucleosome assembly
Blood coagulation	Response to pest/pathogen/parasite	Regulation of catabolism
Hemostasis	Antigen processing, exogenous antigen via MHC-II	Regulation of proteolysis and peptidolysis
Ectoderm development		
Histogenesis	Antigen presentation, exogenous antigen	Monocarboxylic acid transport
Alcohol metabolism	Antigen processing, endogenous antigen via MHC-I	Melanin biosynthesis
Fatty acid metabolism		Melanin biosynthesis from tyrosine
Proteoglycan metabolism	Response to stress	
Di-, tri-valent inorganic cation	Humoral immune response	Blood coagulation
Homeostasis	Humoral defense mechanism (sensu vertebrata)	Melanin metabolism
Carbohydrate biosynthesis		mRNA cleavage
Secretory pathway	Antigen presentation/endogenous antigen	Antimicrobial humoral response
Aldehyde metabolism	Complement activation	Hemostasis

* EASE score range.

Table 6

HLA Class II Antigen Expression

Gene	Cnj SI	Co SI
MHC Class II		
DRB1	4073	135
DRB4	3984	137
DRB1-0402 allele	3324	85
DRA	3117	69
DRB5	2793	118
DPw3-alpha-1 chain	2043	96
DPB1	1300	67
DQB/DRw6	1168	93
DMA	705	46
DQ alpha 1	683	29
DMB	462	85
DRB3	260	33
Reference		
GAPDH	5487	8365
β-Actin	4456	4204

Table 7

Relative Levels of Message for Connexin in the Corneal Epithelium as Calculated from Ct Values Obtained by Real-Time PCR or from the Microarray SIs

		Real-Time PCR			Microarray		
Target	**Human Genome C_t**	**C_t**	**ΔC**	**$2^{-\Delta Ct}$**	**$SI/SI^{C\times43}$**	**SI**	**P Status**
Connexin 43	25.36	26.14	0.00	1.00	1.00	4,573.27	PPP
Connexin 31.1	25.99	28.67	2.53	0.17	0.12	534.53	PPP
Connexin 31	25.07	29.08	2.94	0.13	0.09	413.07	PPP
Connexin 36	26.56	>40.00	>15.86	0.00	*	83.57	AAA
Connexin 59	24.67	38.96	12.82	0.00	*	55.50	AAA
Connexin 37	25.28	37.26	11.12	0.00	*	34.10	APA
Connexin 50	23.99	>40.00	>15.86	0.00	*	28.77	AAA
Connexin 32	26.52	39.05	12.91	0.00	*	28.00	AAA
Connexin 40	25.17	38.78	12.64	0.00	*	13.87	AAA

P Status: present or absent in experiments 1, 2, and 3 respectively.

*Not relevant (transcript is absent).

Invest Ophthalmol Vis Sci. Author manuscript; available in PMC 2010 July 26.

Table 8

SIs and Co/Cnj Ratios for Corneal Reductases and Dehydrogenases

Gene	GB Accession	Co	Cnj	Co/Cnj
Reductases				
NQO1/cytochrome b5 red./NAD(P)H menadione reductase 1	NM_000903	8053	734	11.0
Ubiquinol-cytochrome c reductase complex	NM_013387	2446	1952	1.3
NADH-coenzyme Q reductase	NM_004552	1501	1605	0.9
Ubiquinol-cytochrome c reductase binding protein	NM_006294	1413	1542	0.9
Ubiquinol-cytochrome c reductase, Rieske polypeptide 1	BC000649	1411	1508	0.9
Ubiquinol-cytochrome c reductase core protein I	NM_003365	1296	977	1.3
Ubiquinol-cytochrome c reductase hinge protein (UQCRH)	NM_006004	1263	1135	1.1
Dehydrogenases				
Aldehyde dehydrogenase 3A1	NM_000691	11200	3535	3.2
Glyceraldehyde-3-phosphate dehydrogenase	BE561479	10874	7559	1.4
Lactate dehydrogenase A (LDHA)	NM_005566	7174	4339	1.7
NADH dehydrogenase (Ubiquinone) 1, subcomplex unknown	NM_002494	2188	1452	1.5
Lactate dehydrogenase B	BE042354	2164	1346	1.6
NADH dehydrogenase (Ubiquinone) 1 beta subcomplex, 4	NM_004547	2042	1687	1.2
Malate dehydrogenase 1, NAD (soluble) (MDH1)	NM_005917	1408	1479	1.0

GB, GenBank.

Table 9

Expression of DKK Isoforms

Gene	GB Accession	Co	Cnj	Co/Cnj
DKK1	NM_012242.1	17.4	18.6	0.9
DKK2	NM_014421.1	11.5	4.5	2.6
DKK3	**NM_013253.1**	**2311.3**	**64.1**	**36.0**
DKK4	NM_014420.1	71.6	100.3	0.7

Bold, significant expression. GB, GenBank.

Table 10

Keratin Gene Expression Levels in Human Cornea and Conjunctiva

	K2a	K3	K4	K5	K6	K6b	K6f	K8	K10	K12	K13	K14	K15	K17	K18	K19
Co	95	**1,191**	***708***	13,752	511	176	694	220	1,121	**10,030**	***141***	5,804	***341***	***242***	1,679	***137***
Cnj	174	**21**	***7,173***	8,909	775	425	976	757	1,643	**1,029**	***8,809***	4,338	***3,422***	***1,358***	1,441	***5,965***
R	1.83	**0.02**	***10.1***	0.65	1.5	2.41	1.41	3.44	1.47	**0.10**	***62.4***	0.75	***10.0***	***5.61***	0.86	***43.5***

Corneal keratins (Co/Cnj > 5) and Cnj keratins (Co/Cnj < 0.2) are shown in bold and bold italic, respectively. K1, K7, and K16 (SIs <100) are not shown.